Journal of Materials Science and Nanotechnology
Volume 11 | Issue 1
ISSN: 2348-9812

Research Article Open Access

Carbon Nanocomposites Deposition under Laser Breakdown from Liquid Toluene

II Rakov[1*], NN Mel'nik[2]

[1]Wave Research Center of A.M. Prokhorov General Physics Institute of the Russian Academy of Sciences, 38, Vavilov Street, 119991, Moscow, Russian Federation

[2]Physical Institute of P.N. Lebedeva of the Russian Academy of Sciences, 53, Leninsky Prospect, 119333, Moscow, Russian Federation

[*]**Corresponding Author:** Rakov Ignat, Wave Research Center of A.M. Prokhorov General Physics Institute of the Russian Academy of Sciences, 38, Vavilov Street, 119991, Moscow, Russian Federation, Tel.: +79032358124, E-mail.: ignat.rakov@gmail.com

Citation: II Rakov, NN Mel'nik (2023) Carbonnanocomposites Deposition under Laser Breakdown from Liquid Toluene. J Mater Sci Nanotechnol 11(2): 101

Received Date: July 29, 2023 **Accepted Date:** August 29, 2023 **Published Date:** August 31, 2023

Abstract

Carbon nanocomposites deposition under toluene irradiation through transparent glass by nanosecond infrared laser radiation at ambient conditions was experimentally investigated. The dependence of deposited coatings thickness on the laser pulse duration and absorbed energy amount is revealed. The atomic force microscope, scanning electron microscope and modulation interference microscope are employed to definition deposited films morphology. The average nanocomposites thickness on a glass substrate increases with the number of laser pulses. Raman spectroscopy was used to determine allotropic modification of synthesized nanocomposites. Raman spectra analysis confirms the presence of significant amount sp3 fraction and some sp2 fraction.

Keywords: Laser Breakdown; Carbon Nanocomposites; Laser Deposition

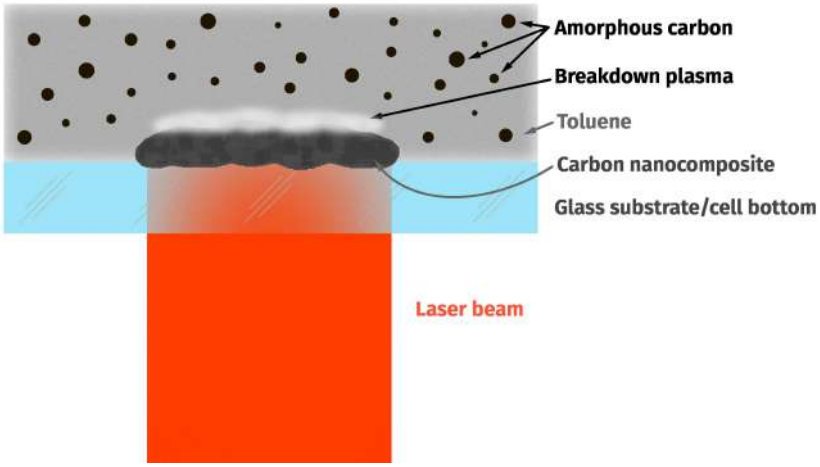

Figure

Introduction

Solid amorphous carbon coatings have been the focus of attention over the past decades. Such nanocomposites can serve as ideal wear-resistant coatings due to their composition, high hardness and low coefficient of friction. Potential applications include mechanical engineering (hardening of various components operating in extreme conditions), medicine (development of biocompatible coatings), microelectronics, and other fields [1-4].

The most common and investigated method of creating diamond-like (DLC) coatings today is pulsed laser deposition (PLD). Powerful pulsed laser radiation focuses on a carbon-containing target in a vacuum chamber. The material evaporates from the target in a plasma plume containing carbon atoms and ions. Evaporating material falls on a substrate (for example, a silicon wafer) located at a certain distance from the target. An important characteristic of the deposited films is the presence of sp^3 and sp^2 allotropic modifications of carbon in it. The first bond type corresponds to the metastable diamond phase, and the second - to stable graphite. Their ratio in deposited film may vary depending on the experimental parameters and external conditions [5]. This process can occur both in ultrahigh vacuum and in the presence of a background gas [6,7]. With an increase in the film density, a transition is observed from amorphous carbon (a -C) to diamond-like carbon (DLC) and tetrahedral amorphous carbon (ta - C) [8].

Also known are works on the synthesis and modification of various allotropic states of carbon using laser radiation. In particular, the authors [9] use the first harmonic of a picosecond Nd:YAG laser to reduction of graphite oxide (GO) to graphene. This method allowed creating electrically and thermally conductive graphene domains in the insulating GO substrate. In [10] demonstrated that laser-assisted SiC decomposition can result in a manifold of graphene structures depending on the irradiation conditions. In particular, graphene formation, at nearly ambient conditions, can take place in various forms resulting in SiC particles covered by few-layer epitaxially grown films, and particles with a progressively increasing thickness of the graphitized layer, reaching eventually to free-standing 3D graphene froths at higher irradiation doses. Authors [11-13] demonstrated laser technology application for carbon nanostructures generation, namely localized heating, multiphoton lithography, tip-enhanced optical near--field effect, polarization, ablation, resonant excitation, precise energy delivery, and mask- free direct patterning. Rapid single-step fabrication of graphene patterns was achieved using laser directing writing. Parallel integration of single-walled carbon nanotubes was realized by making use of tip-enhanced optical near-field effect.

In previous works authors [11,14] carried out the deposition of diamond-like films from liquid aromatic carbons (benzene, cumene, and toluene) using a copper vapor laser. In the range of laser radiation energy density from 0.5 to 1.5 J/cm^2, the transparent substrate was ablated to a depth of the order of 0.1-0.2 μm with simultaneous deposition of the DLC.

The fundamental difference is the use of another source of laser radiation. Using in this work the ytterbium laser it's supposed to avoid the glass substrate itself etching due to different absorption in comparison with a copper vapor laser. In other words, when operating in the infrared wavelength range, the risk of etching of the substrate itself is significantly reduced due to the lower absorption by the nanocomposite at these wavelengths. A pulsed laser radiation source is used, in which the pulse energy is an order of magnitude higher than that of CW (continuous wave) lasers. Thus the intensity of laser breakdowns and the local temperature gradient at the liquid-substrate interface increase. The intensity profile of the laser beam in the case of a copper vapor laser is "flat--top", while the laser profile used in the present work has a beam profile close to Gaussian. In addition, in this work the number of emitted laser pulses is controlled, and it is also possible to control the movement of laser beam by a galvanic-optical mirror system.

Moreover, authors of the previous work did not observe optical breakdowns on amorphous carbon particles. This is probably due to laser beam high brightness (510.6 nm), especially in the region of deposition.This work is devoted to experimental study of the morphology and allotropic composition of carbon nanocomposites deposited on a glass substrate under laser irradiation of an aromatic hydrocarbon (toluene).

Experimental Setup

The deposition of carbon from toluene on the surface of a glass slide occurred under the influence of high-intensity laser radiation. Toluene was decomposed by a pulsed ytterbium fiber laser operating in the wavelength range of 1060–1070 nm with a frequency of 20 kHz, pulse duration of 100 ns and fluence of the order of 6–7 J/cm^2. The interface irradiating process between glass and toluene is accompanied by intense formation of gas bubbles. Their size increases to 100-200 microns at a distance of about 1-2 mm from the glass surface. To ensure the removal of gas bubbles arising during the toluene decomposition, laser radiation was introduced into a cell from below. Thus, the bubbles left the working area, not interfering with the absorption and formation of the carbon nanocomposites. The experimental setup is shown in Figure 1.

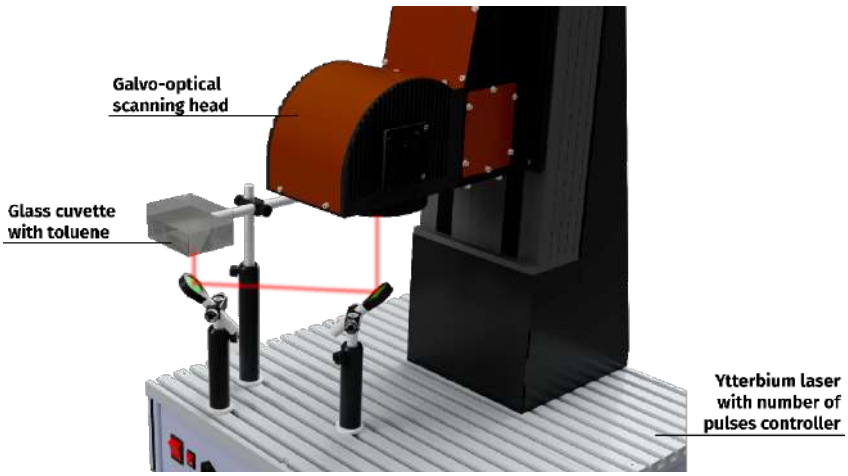

Figure 1: Experimental setup on laser-assisted deposition of carbon nanocomposites from liquid toluene.

The radiation was focused by the F-Theta lens, and the beam was moved by a galvanic-optical mirror system. The search for the optimal parameters of laser radiation showed that the most stable and repetitive result is achieved at an energy of about 0.5 mJ per pulse. Exceeding this threshold energy value destroys the glass surface and ends the coating deposition process.

To determine the rate of carbon nanocomposite formation, as well as its size depending on the absorbed energy, the beam moved along a matrix of dots (diameter about 70 μm, distance between points 250 μm), in each of which a certain number of pulses were absorbed. The following values were selected - 10, 100, 1000, 5000 and 10000 pulses per point. It was found that the extreme values did not make a significant contribution, since at 10 pulses the amount of energy is clearly not enough to form a carbon film, and at 10,000 pulses the glass substrate itself is irreversibly damaged.

The composition of the deposited nanocomposites and the initial carbon precipitated during toluene decomposition was studied using Raman spectroscopy (U1000 spectrometer). For excitation, a CW argon laser with a wavelength of 457.9 nm was used. The thickness and morphology of carbon films was determined using an Amphora MIM-321 (CW 405 nm) modulation interference microscope and a Nanopics 2100 KLA-Tencor scanning atomic force microscope. A general view of diamond-like coatings on the substrate surface was performed using a JEOL JSM-5910LV scanning electron microscope with primary beam acceleration at 20 keV and an incidence angle of 15^0.

Results

After nanocomposites deposition the glass substrate was cleaned of amorphous carbon particles and toluene for subsequent optical studies. Cleaning was carried out mechanically and in an ultrasonic bath with ethanol. Such processing did not affect nanocomposites stability and morphology which indicates a sufficiently high coating adhesion to the substrate surface. Initial estimation of the deposited nanocomposite thickness as a function of laser pulses number was carried out using interference spectroscopy. Nanocomposites appearance and their profilograms are shown in Figure 2. The profile was recorded at the composite-substrate (glass) interface.

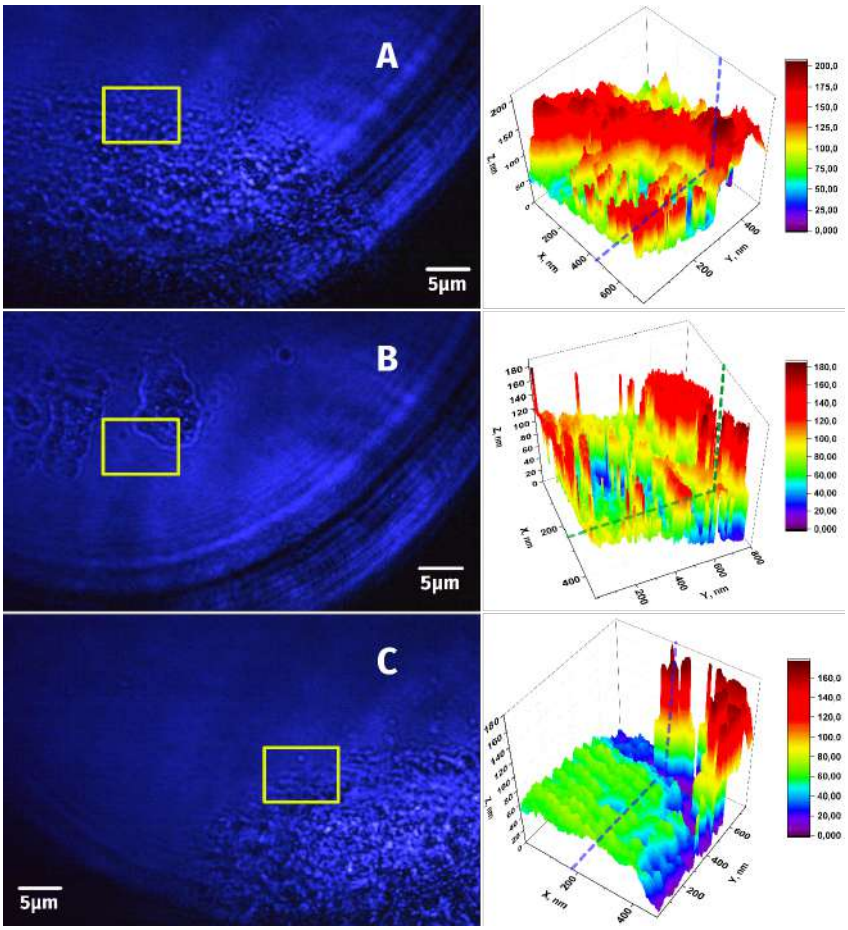

Figure 2: Images and profilograms of carbon nanocomposites deposited at various numbers of laser pulses: 100 pulses/point (A), 1000 pulses/point (B) and 5000 pulses/point (C)

Comparing Figure 2A and Figure 2C one can see that increasing pulses number leads to the change on the deposited coating thickness. The nanocomposite thickness at a small number of pulses (100 pulses/point) is about 150-160 nm, while at 5000 pulses/point it exceeds 200 nm. The Z-axis resolution is limited by the laser diode operating wavelength of the interference microscope itself (405 nm). In addition, a more accurate assessment of the thickness of the deposited coatings performed using an atomic force microscope. The profiles of nanocomposites deposited at different values of absorbed energy are presented in Figure 3.

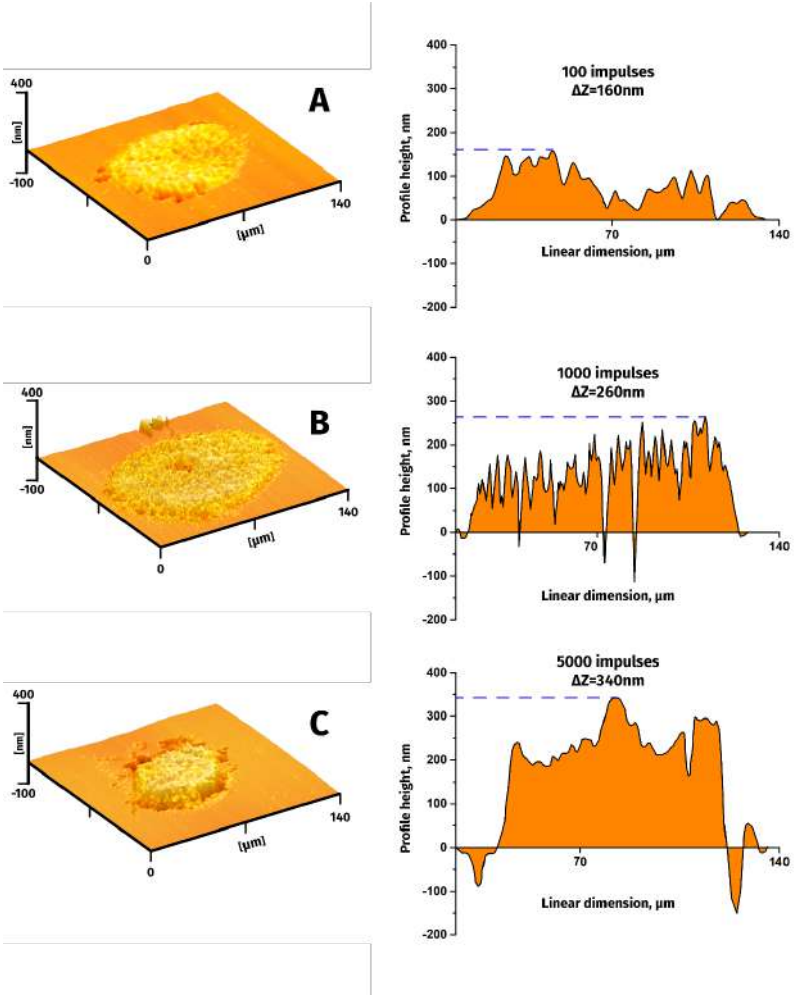

Figure 3: AFM images of nanocomposites synthesized with a different pulse number: 100 pulses/point (A), 1000 pulses/point (B) and 5000 pulses/point (C)

Comparing AFM images the difference on deposited nanocomposites thickness is clearly visible. Already at 100 pulses per point, the film thickness is about 160 nm. In this case, the deposition time is equal to beam standing time at the point and is 10 μs. An increase in laser pulses number per point leads to change of the deposited coating thickness. For 5000 pulses per point it's already about 330 nm and the deposition time is 50 ms.It is also clearly seen that etching of the substrate in the process of increasing the thickness of the deposited coating is not observed. The carbon film is located on the glass surface and remains transparent to IR radiation (Figure 3A and B). Figure 3C shows that the substrate at the boundary of the deposited coating began to break down. This is probably due to the achievement of a critical film thickness at which the nanocomposite begins to absorb laser radiation and heats up significantly. Such conclusions are supported by the analysis of images of deposited nanocomposites performed by using a scanning electron microscope (Figure 4).

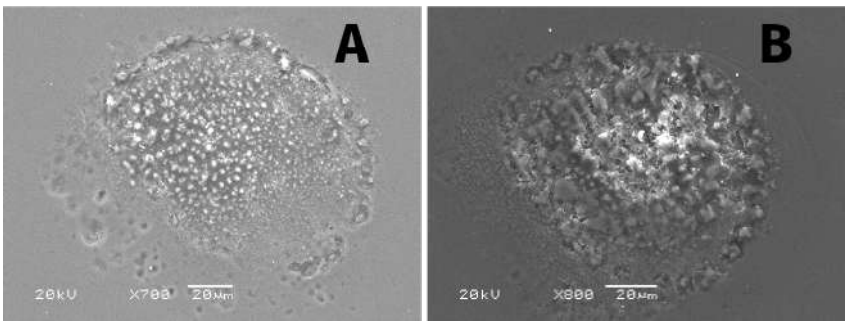

Figure 4: SEM images of carbon nanocomposites: 100 pulses/point (A) and 5000 pulses/point (B).

It is clearly seen that the carbon nanocomposite has a somewhat fragmented structure at a lower amount of absorbed energy (Figure 4A). Formation of separate regions at the beam periphery is observed in this case. Increasing the number of pulses leads to formation of a fairly uniform configuration with a maximum in the central region. In addition, in some cases, the beginning process of base destruction (Figure 4B) is noticeable. Apparently it is due to a local excess of the thickness and density of the nanocomposite. As a result of which more efficient absorption of the laser radiation by the coating itself occurs.

The composition of the deposited nanocomposites was studied using Raman spectroscopy. CW argon laser with a wavelength of 457.9 nm was used for excitation. The Raman spectra of carbon nanocomposites of various thicknesses are shown in Figure 5. It is important to note that these spectra are the result of the difference between two signals: the coating itself and the substrate. Initial spectrum of the glass base itself is shown for comparison.

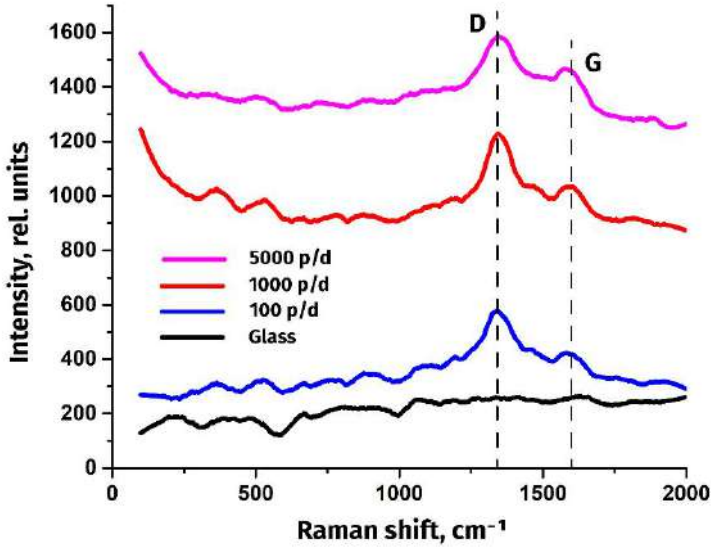

Figure 5: Raman images of nanocomposites synthesized with a different pulse number: 100 pulses/point (A), 1000 pulses/point (B) and 5000 pulses/point (C).

The Raman spectra of all three carbon nanocomposites are clearly dominated by two peaks: in the region of 1350 cm^{-1} and 1600 cm^{-1}. According to [15,16] these peaks correspond to the sp3 and sp2 allotropic forms of carbon in the composite. Apparently, fluctuations in the region of 1350 cm^{-1} correspond to the diamond fraction (D) in the structure of the deposited coating and the line in the region of 1600 cm^{-1} corresponds to graphite (G). The signal in the region of 500 cm^{-1} is also responsible for the sp^2 vibrations of carbon atoms which are characteristic of chemical bonds in amorphous carbon. Also, with an increase in the thickness of the deposited nanocomposites, an increase in the intensity of scattered radiation in the Raman spectra is observed. It should also be noted that the presence of closely spaced sp^3 and sp^2 modifications in carbon samples leads to the appearance of photoluminescence in the visible region [17]. It can be seen that as the thickness of the deposited nanocomposites increases, the Raman spectra shift upward, which may correspond to an increase in the thickness of the photoluminescent substrate. Such an effect is apparently related to the graphitization of the samples, which is also evidenced by the broadening of the peak in the region of 1600 cm^{-1}.

We also compared the Raman spectra of the carbon nanocomposite and amorphous carbon formed during laser irradiation of toluene. Such a comparison is necessary to make sure that the observed in Figure 5. allotropic modifications of carbon are not decomposition products of toluene. As a sample of amorphous carbon we used the precipitate that remained in the cuvette at the end of the deposition process and dried on a silicon plate. Comparison of Raman spectra of nanocomposite and amorphous carbon is shown in Figure 6.

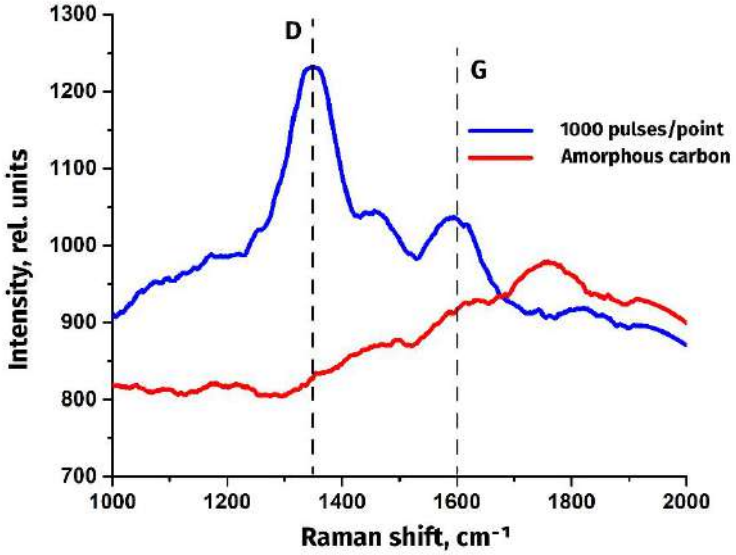

Figure 6: Raman spectra of the nanocomposite (blue line) and amorphous carbon (red line) formed in the cell as a result of laser decomposition of toluene.

It can be seen that the Raman spectrum of amorphous carbon lacks peaks corresponding to the sp^3 and sp^2 allotropic modifications. A small peak is observed in the region of 1800 cm^{-1}, most likely related to the hydrocarbon functional group (CH) of toluene, which evaporated during the preparation of the carbon deposit sample on the silicon plate. Thus, we can conclude that diamond and graphite, which form the nanocomposite, are formed exclusively on a glass substrate, and under strictly defined conditions. The action of laser radiation on methylbenzene leads to formation of amorphous carbon particles, which further participate in the process of nanocomposite deposition.Also Raman spectra of the synthesized nanocomposite and the spectrum of disordered carbon presented in [18] were compared. The authors of this publication conclude that there are nanodiamonds in the samples. However, synthesis method is fundamentally different from that presented in this work and consists in heating a mixture of carbon-containing gas, nitrogen and organic matter to 500°C at a pressure of 1000 bar. Comparison of the spectra is shown in Figure 7.

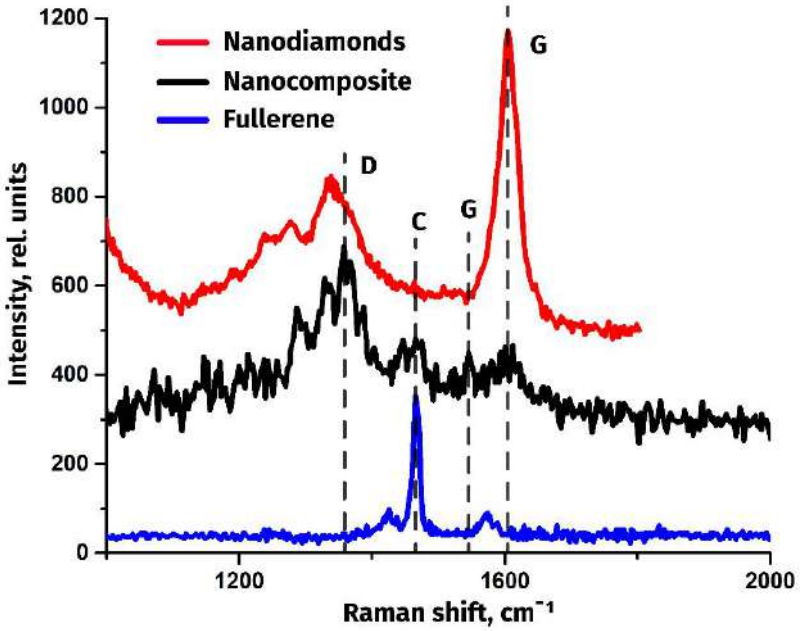

Figure 7: Comparison of Raman spectra: nanocomposite (averaging over three samples, black line), fullerene and nanodiamonds [18].

It is important to note that the samples were synthesized using completely different techniques, but their Raman spectra have a number of common features. For example, one can see almost complete coincidence of the positions of the characteristic D and G peaks both in the composition of the nanocomposite deposited from toluene and in nanodiamonds. In addition, the coincidence of peaks in the region of 1560 cm-1 is observed when comparing the Raman spectra of fullerene and carbon nanocomposite. According to the literature data, this behavior may correspond to the presence of the sp2 allotropic modification of carbon (fullerene) in the nanocomposite structure [19].

Discussion

At the initial stage laser radiation is absorbed by impurities contained in liquid toluene. As a result rare optical breakdowns of low intensity are observed, near which the process of toluene decomposition begins. One of the decomposition products is amorphous carbon particles, which consist of pure carbon with a small content of high-temperature hydrocarbons [20]. Further most of the laser radiation is absorbed precisely on these particles, as a result of which they are significantly heated. Strong heating leads to the formation of a vapor-gas shell around the amorphous carbon particles. Inside this shell in turn a high-intensity plasma is observed. Formation mechanism of such optical breakdowns on individual particles, as well as some properties of such a plasma, are described in [21,22]. Table 1 presents the values of thermal conductivity and thermal diffusivity of all materials involved in the synthesis of carbon nanocomposites.

Material	Coefficient	
	Thermal conductivity (at 20°C), W/m*K	Thermal diffusivity, m^2/s
Toluene	0,113	$6,9*10^{-6}$
Vapors of toluene	0,009	$2,86*10^{-5}$
Diamond	1000-2600	$\sim 2,5*10^{-4}$
Graphite	280-2000	$1,22*10^{-6}$
Amorphous carbon	3-8	$2,1*10^{-4}$
Glass	1,15	$3,4*10^{-7}$

Table 1: Values of heat and thermal diffusivity of materials

Thus a nonequilibrium process is observed in a thin layer of liquid at the glass-toluene interface. This process is accompanied by the dissociation of toluene, the formation of a breakdown plasma, active gas formation, high temperature and pressure. The difference of almost three orders of magnitude between the thermal conductivity of glass and toluene vapor (1.15 and 0.009 $W^*m^{-1*}K^{-1}$, respectively) leads to the formation of a large temperature gradient at the interface. Consequently, when the gas-vapor shell collapses, some strongly heated amorphous carbon particles fall on a conditionally cold glass substrate and instantly solidify (harden) on it, forming a carbon nanocomposite.

It should be noted that a more detailed study of the morphology and concentration of amorphous carbon collected as a precipitate after the deposition of the nanocomposite should be carried out separately. This could provide new information about optimizing the process of synthesis of such coatings, help with the selection of parameters of the laser source and deposition modes (for example, with additional cooling or mixing of the solution during irradiation).

In addition, as mentioned earlier, active gas formation was observed during the carbon nanocomposite deposition. Apparently, this gas is hydrogen, which was formed during the toluene decomposition ($C_6H_5CH_3$) under the action of laser radiation. A similar process is described in [23].

Another feature can be traced in the analysis of images obtained with a transmission electron microscope (Figure 4). The introduction presents [10], the authors of which synthesized various graphene structures on the surface of silicon carbide particles by laser action with different radiation parameters. It is shown that an increase in the irradiation time leads to an increase in the thickness of the graphite layer, which subsequently transforms into foam graphene. A comparison of the TEM image of the surface of the synthesized carbon nanocomposite with the SEM image of graphene foam on the surface of silicon carbide is shown in Figure 8.

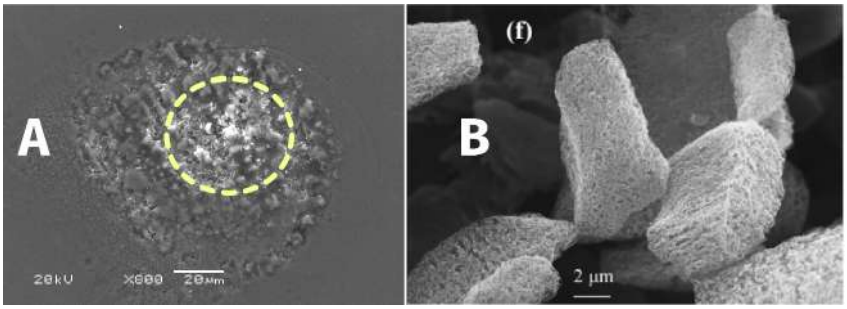

Figure 8: SEM image of the surface of a carbon nanocomposite (**A**) (5000 pulses/point) and three-dimensional graphene froth (B) [10].

It can be seen that a region differing in contrast is concentrated in the central part of the carbon film. It is important to note that similar areas are also present in the case of a smaller amount of absorbed energy (Figure 4A), but they are much smaller and scattered over the surface of the nanocomposite. This feature can be attributed to the formation of regions, presumably consisting of graphene froth, in some cases during the deposition of a diamond-like film under the action of laser radiation on toluene. An allotropic modification corresponding to graphene is observed in the Raman spectra of nanocomposites (Figure 7), however, it is difficult to draw a conclusion regarding its appearance due to the low resolution of SEM images.

Conclusions

Thus in this work the dependence of the morphology and allotropic composition of carbon nanocomposites deposited upon irradiation of methylbenzene with nanosecond pulsed infrared radiation on the number of absorbed laser pulses was experimentally studied for the first time. It is shown that during the irradiation of a cell with toluene through a transparent window, the deposition of a carbon film is initiated at the interface (glass-toluene), which contains several allotropic modifications, mainly diamond, fullerene and graphite (sp^3 and sp^2) according to Raman spectroscopy data. It was also found that changing the number of laser pulses absorbed at one point from 1000 to 5000 leads to an increase in the thickness of the deposited carbon nanocomposite by 2.5 times (from 160 to 340 nm). A further increase in the number of laser pulses leads to the destruction of the surface of the glass substrate in the region of deposition.

It is shown that the allotropic composition, namely the content of graphite (sp^2) in a diamond-like film, depends on the amount of absorbed energy. As the number of pulses increases and the carbon nanocomposite grows, the process of its graphitization is initiated. The close location of the sp^3 and sp^2 bonds causes the appearance of photoluminescence in the visible region, which increases with the growth of the composite.

Acknowledgement

The work was supported by the Scholarship of the President of the Russian Federation for young scientists SP-1006.2021.1

References

1. Bonaccorso F et al. (2015) Graphene, related two-dimensional crystals, and hybrid systems for energy conversion and storage // Science (80). 347: 6217.

2. Shao Y. et al. (2010) Graphene Based Electrochemical Sensors and Biosensors: A Review // Electroanalysis 22:1027–1036.

3. Mittal G. et al. (2015) A review on carbon nanotubes and graphene as fillers in reinforced polymer nanocomposites // J. Ind. Eng. Chem 21: 11–25.

4. Jo Gunho et al. (2012) The application of graphene as electrodes in electrical and optical devices // Nanotechnology. IOP Publishing . 23: 112001.

5. Bäuerle D (2000) Liquid-Phase Deposition, Electroplating 449-58.

6. Vaziri MR Rashidian (2010) Microscopic description of the thermalization process during pulsed laser deposition of aluminium in the presence of argon background gas // J. Phys. D. Appl. Phys 43: 425205.

7. Robertson J (2002) Diamond-like amorphous carbon // Mater. Sci. Eng. R Reports 37: 129-81.

8. Bonelli M et al. (2002) Structure and mechanical properties of low stress tetrahedral amorphous carbon films prepared by pulsed laser deposition // Eur. Phys. J. B 25: 269-80.

9. Trusovas R et al. (2013) Reduction of graphite oxide to graphene with laser irradiation // Carbon N. Y 52: 574-82.

10. Antonelou A, Dracopoulos V, Yannopoulos SN (2015) Laser processing of SiC: From graphene-coated SiC particles to 3D graphene froths // Carbon N. Y. Pergamon 85: 176-84.

11. Simakin AV, Shafeev GA, Loubnin EN (2000) Laser deposition of diamond-like films from liquid aromatic hydrocarbons // Appl. Surf. Sci 154: 405-10.

12. Yang SB et al. (2011) Recent advances in hybrids of carbon nanotube network films and nanomaterials for their potential applications as transparent conducting films // Nanoscale 3: 1361.

13. Duy LX et al. (2018) Laser-induced graphene fibers // Carbon N. Y. Pergamon 126: 472-9.

14. Simakin AV, Obraztsova ED, Shafeev GA (2000) Laser-induced carbon deposition from supercritical benzene // Chem. Phys. Lett 332: 231-5.

15. Dennison HR, Spectroscopy S (1996) Raman Spectroscopy of Carbon Materials 11: 1.

16. Wang Y, Alsmeyer DC, McCreery RL (1990) Raman Spectroscopy of Carbon Materials: Structural Basis of Observed Spectra // Chem. Mater. American Chemical Society 2: 557–63.

17. Karavanskiĭ VA, Mel'nik NN, Zavaritskaya TN (2001) Preparation and study of the optical properties of porous graphite // JETP Lett. Springer 74: 186.

18. Simakov S (2010) Metastable Nanosized Diamond Formation from Fluid Systems // Nat. Preced.

19. Wu J Bin et al. (2018) Raman spectroscopy of graphene-based materials and its applications in related devices // Chemical Society Reviews. Royal Society of Chemistry 47: 1822–73.

20. Toyota K et al. (2001) Analysis of products from breakdown of liquid benzene, toluene and cyclohexane caused by Nd3+:YAG pulsed laser irradiation // J. Photochem. Photobiol. A Chem. Elsevier 141: 9-16.

21. Chaudhary K, Rizvi SZH, Ali J (2016) Laser-Induced Plasma and its Applications // Plasma Science and Technology - Progress in Physical States and Chemical Reactions.

22. Serkov AA et al. (2016) Influence of laser-induced breakdown on the fragmentation of gold nanoparticles in water // Quantum Electron 46: 713-8.

23. Simakin AV et al. (2019) The Effect of Gold Nanoparticle Concentration and Laser Fluence on the Laser-Induced Water Decomposition // J. Phys. Chem. B. American Chemical Society 123: 1869-80.